Available online at www.sciencedirect.com
ScienceDirect
Journal of Hazardous Materials 146 (2007) 39–50
Journal of Hazardous Materials
www.elsevier.com/locate/jhazmat

Adsorption of platinum (IV), palladium (II) and gold (III) from aqueous solutions onto L-lysine modified crosslinked chitosan resin

Kensuke Fujiwara, Attinti Ramesh *, Teruya Maki, Hiroshi Hasegawa, Kazumasa Ueda *

Department of Chemistry and Chemical Engineering, Graduate School of Natural Science and Technology, Kakuma, Kanazawa University, Kanazawa 920-1192, Japan

Received 28 August 2006; received in revised form 21 November 2006; accepted 23 November 2006
Available online 30 November 2006

Abstract

Crosslinked chitosan resin chemically modified with L-lysine has been used to investigate the adsorption of Pt(IV), Pd(II) and Au(III) from aqueous solutions. Batch adsorption studies were carried out with various parameters, such as initial metal ion concentration, contact time, pH and temperature. The maximum adsorption capacity was found at pH 1.0 for Pt(IV), at pH 2.0 for Au(III) and Pd(II). Langmuir and Freundlich isotherm models were applied to analyze the experimental data. The best interpretation for the experimental data was given by the Langmuir isotherm and the maximum adsorption capacity was found to be 129.26 mg/g for Pt(IV), 109.47 mg/g for Pd(II) and 70.34 mg/g for Au(III). The kinetic data was tested using pseudo-first-order and pseudo-second-order kinetic models. Kinetic data correlated well with the pseudo-second-order kinetic model, indicating that the chemical sorption was the rate-limiting step. Thermodynamic parameters like Gibbs free energy (ΔG°), enthalpy (ΔH°) and entropy (ΔS°) were evaluated by applying the Van't Hoff equation. The thermodynamic study indicated that the adsorption process is spontaneous and exothermic in nature. The desorption studies were carried out using various reagents. The maximum percent desorption of precious metal ions were obtained when the reagent 0.7 M thiourea–2 M HCl was used.
© 2006 Elsevier B.V. All rights reserved.

Keywords: Crosslinked chitosan resin; L-Lysine; LMCCR; Pt(IV); Pd(II); Au(III); Adsorption; Thermodynamics; Kinetics

1. Introduction

Precious metals are widely used in industry, agriculture and medicine, because of their specific physical and chemical properties. Economically, the precious metals have been historically important as currency, and remain important as investment commodities. Gold, silver, platinum and palladium are internationally recognized as forms of currency under ISO 4217. Hence, the value and scarcity of precious metals like, gold, silver, platinum and palladium, it's necessary to treat the waste aqueous solutions and try to recover them economically. Many studies have been recently focused on the extraction and separation of precious metals due to both increasing industrial need for these metals and their limited sources. The conventional methods for the removal of metal ions from water and wastewater include oxidation, reduction, precipitation, membrane filtration, ion-exchange and adsorption. Among the all above methods adsorption is highly effective and economical.

Biopolymers have recently received a great deal of attention due to the fact that they represent renewable resources and are more environmental friendly than conventional materials. Chitosan, poly(D-glucosamine), is obtained by deacetylation of chitin which is the most abundant polysaccharide after cellulose on the earth. Chitosan is non-toxic, hydrophilic, biodegradable, biocompatible and anti-bacterial, which has led to very vast range of applications in the biomedical field, cosmetic, food and textile industries [1]. In a previous research, it was demonstrated that chitosan is an excellent adsorbent for the removal of metal ions, dyes and proteins. Muzzarelli and Rocchetti [2] reported that through the hydroxyl group and amino group, chitosan can form the stable chelate compounds with many transition metal ions. The presence of amino groups in the chitosan chain increases the adsorption capacity of chitosan to that of chitin, which only has a small percentage of amino groups [3]. The presence of amino groups in chitosan besides hydroxyl groups is highly advantageous for conducting modification reactions. However, the amine groups are easily protanated in acidic

* Corresponding authors. Tel.: +81 76 234 4792; fax: +81 76 234 4792.
E-mail addresses: attintiram@yahoo.com (A. Ramesh), kueda@t.kanazawa-u.ac.jp (K. Ueda).

0304-3894/$ – see front matter © 2006 Elsevier B.V. All rights reserved.
doi:10.1016/j.jhazmat.2006.11.049

solutions [4]. Hence, the protanation of these amino groups may cause electrostatic attraction of anionic compounds, including metal anions or anionic dyes. Indeed, nitrogen atoms hold free electron doublets that can react with metal ions [5].

However, chitosan can be dissolved in acid media and its applications are limited. Due to overcome these problems chitosan was modified with different crosslinking agents. Several crosslinkers such as glutaraldehyde [6–8], epichlorohydrin [9], ethyleneglycoldiglycidylether [10,11] and oxidized β-cyclodextrin [12] have been used to modify the chitosan for metal ion removal. In order to increase the sorption selectivity of metal ions a great number of chitosan derivatives have been obtained by grafting new functional groups on the chitosan backbone. Hence, poly(ethylenimine) [13,14], thiourea [15], thiourea/rubeanic acid [16] and poly(ethylenimine)/thiourea [4] have been grafted on chitosan through glutaraldehyde linkage. The selectivity for a specific metal ion depends on what kind of complexing agent is introduced into the polymeric chain. According to the theory of hard and soft acids and bases (HSAB) defined by Pearson, metal ions will have a preference for complexing with ligands that have more or less electronegative donor atoms. Chelating agents with N and S groups are highly efficient for the selective sorption of precious metal ions. Several chelating ligands such as 3,4-diamino benzoic acid [17], *N*-methyl-D-glucamine [18], ethylene diamine [19], 2[-bis-(pyridylmethyl)aminomethyl]-4-methyl-6-formylphenol [20] were used to functionalize the crosslinked chitosan for adsorption of metal ions. There have been no reports to date for the adsorption of precious metal ions onto chitosan and lysine as a spacer group, crosslinked with EDGE and PEI.

In the present investigation we synthesized L-lysine methyl ester hydrochloride with crosslinked chitosan resin for the removal of Pt(IV), Pd(II) and Au(III) from aqueous solutions. The experimental studies were carried out by batch adsorption studies. This study also focuses on the study of Pt(IV), Pd(II) and Au(III) desorption by various acids and reagents. Fourier transform infrared spectroscopy (FT-IR) was used to record the functional groups on the modified/unmodified crosslinked chitosan resin, respectively.

2. Experimental

2.1. Chemicals

All the chemicals used were of analytical reagent grade. E-Pure (EP) water was used throughout the experimental studies. Crosslinked chitosan resin (chitopearl CS-03) was obtained from Fujibo holings Inc., Tokyo, Japan. L-lysine methyl ester hydrochloride (Aldrich), AAS grade Pt(IV), Pd(II) and Au(III) standard solutions, (Kanto chemicals, Japan, 1 mg/ml) HOBt, DCC, DMF, *n*-methyl morpholine, thiourea, HCl, NaOH and buffer solutions (Wako chemicals, Japan) were used. Working standards were prepared by progressive dilution of standard Pt(IV), Pd(II) and Au(III) solutions using EP water. The physicochemical parameters such as ion exchange capacity, surface area, particle size and specific weight of chitoperal CS-03 were found to be 1.73 meq/g, 19.8 m^2/g, 100–200 μm and 0.70 g/ml, respectively. Ion exchange capacity of chitoperal CS-03 was studied according to the method described by Takeda et al. [29].

2.2. Instrumentation

Atomic emission spectrophotometer (ICP-AES, Perkin Elmer) was used to determining the concentration of Pt(IV), Pd(II) and Au(III). Fourier transform infrared spectrometry (Perkin-Elmer) was used to analyze the functional groups in the adsorbent. The transmission spectrum was acquired at a 64 scans with 4 cm^{-1} resolution and the spectrum was corrected with KBr background. A pH meter (Horiba, F-52) was used for pH measurements. Scanning electron microscopy (SEM, Hitachi, S-4500) was used to analyze the surface morphology of the CCR and LMCCR. Temperature controlled bio-shaker (Taitec, BR-30L) was used for agitating the sample solutions. Surface area measurements were carried out using the Brunauer–Emmett–Teller (BET) equation on a Quantachrome NOVA 2000 apparatus.

2.3. Synthesis of L-lysine modified crosslinked chitosan resin

The synthesis of L-lysine modified crosslinked chitosan (LMCCR) was carried out in three steps, as show in Fig. 1. In step 1, 6.0 g of crosslinked chitosan resin (CCR) was taken into three necked round bottom flask, and then 50 ml of 50% glyoxylic acid solution and small amount of EP water were added. The resin was stirred at 160 rpm for 24 h at 25 °C. The product was filtered and washed with EP water. In step 2, the resin from step 1 was transferred into a three-necked round bottom flask. To this added 300 ml of DMF solution, 55 mmol of DCC, 100 mmol of HOBT, L-lysine methyl ester hydrochloride and *n*-methyl morpholine at 0 °C. The resin was stirred for 1 h at 160 rpm and continued the agitation for 24 h at 25 °C. Then, the solid product was filtered and washed with methanol and EP water (1:1) solution. Finally, the product from step 2 was transferred into a three necked round bottom flask and added 500 ml of 0.02 M NaOH solution at 25 °C. Then, the product was stirred for 24 h at 160 rpm, filtered and washed with methanol and dichloromethane (1:1) solution.

2.4. Adsorption studies

Batch adsorption experiments were conducted in 100 ml stoppered reagent bottles. Then 30 ml aliquots of aqueous solution containing various concentrations of Pt(IV), Pd(II) and Au(III) were introduced into 100 ml reagent bottles and the solution pH was adjusted to the desired value by adding hydrochloric acid or ammonia solution. To this weighed amount (0.1 g) of CCR or LMCCR was placed and the bottles were shaken at 100 rpm at room temperature (30 ± 1 °C) using a mechanical shaker for prescribed length of time to attain equilibrium. After filtration, the concentration of Pt(IV), Pd(II) and Au(III) were analyzed using ICP-AES. The effect of Pt(IV), Pd(II) and Au(III) metal ion concentration (10–400 mg/l), contact time (0.1–7 h), solution

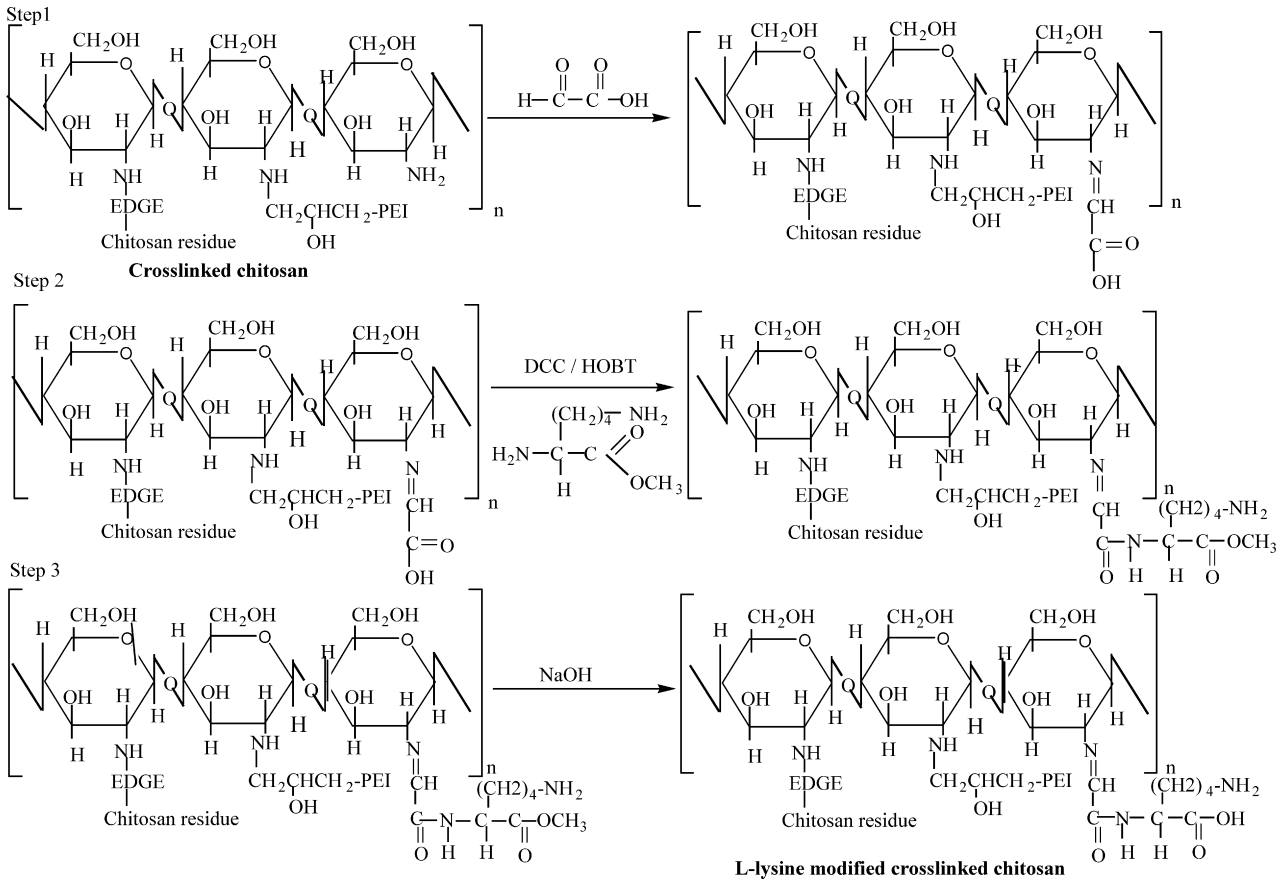

Fig. 1. Scheme for the synthesis of L-lysine modified crosslinked chitosan.

pH (1–10) and temperature (30–50 °C) were studied. Blank solutions were treated similarly (without adsorbent) at the recorded concentration by the end of each operation was taken as the initial one.

2.5. Adsorption isotherm models

The adsorption data of Pt(IV), Pd(II) and Au(III) on CCR or LMCCR were analyzed in terms of Freundlich [21] and Langmuir isotherm models [22]. Freundlich isotherm equation $X/m = k_F C_e^{1/n}$ can be written in the linear form as given below.

$$\log \frac{X}{m} = \log k_F + \frac{1}{n} \log C_e \quad (1)$$

where X/m, and C_e are the equilibrium concentrations of Pt(IV), Pd(II) and Au(III) in the adsorbed (mg/g) and liquid phases (mg/l), respectively. k_F and n are the Freundlich constants which are related to adsorption capacity and intensity, respectively. These constants can be calculated from the slope and intercept of the linear plot, with $\log(X/m)$ versus $\log C_e$.

The Langmuir adsorption isotherm equation $X/m = Q_m k_L C_e/(1 + k_L C_e)$ on linearization becomes

$$\frac{C_e}{X/m} = \frac{C_e}{Q_m} + \frac{1}{Q_m k_L} \quad (2)$$

where Q_m and k_L are the Langmuir constants which are related to the adsorption capacity and energy of adsorption, respectively and can be calculated from the intercept and slope of the linear plot, with $C_e/(X/m)$ versus C_e.

2.6. Kinetics of adsorption

The kinetics of the adsorption process was studied by carrying out a set of adsorption experiments at constant temperature and monitoring the amount adsorbed with time. The adsorption kinetic data of Pt(IV), Pd(II) and Au(III) was analyzed in terms of pseudo-first-order [23] pseudo-second-order kinetic equations [24,25], intraparticle diffusion model [26] and liquid film diffusion model [27]. Assuming the pseudo-first-order kinetics, the rate of the adsorptive interactions can be calculated by using the Lagergren equation.

$$\log(q_e - q_t) = \log q_e - \frac{k_1}{2.303} t \quad (3)$$

where q_e and q_t are the amounts of adsorbed Pt(IV), Pd(II) and Au(III) (mg/g) at equilibrium and time t, respectively, and k_1 (min^{-1}) is the rate constant of pseudo-first- order adsorption. The q_e and rate constant, k_1 were calculated by plotting the log $(q_e - q_t)$ versus t.

The pseudo-second-order equation can be written as

$$\frac{dq_t}{dt} = K_2 (q_e - q_t)^2 \quad (4)$$

where k_2 (g/mg min) is the rate constant of sorption, q_e is the amount of Pt(IV), Pd(II) and Au(III) adsorbed (mg/g) at equilibrium, and q_t is the amount of the adsorption (mg/g) at any time t. Integrating Eq. (4), using boundary conditions $q_t = 0$ at $t = 0$ and $q_t = q_t$ at $t = t$ gives

$$\frac{1}{q_e - q_t} = \frac{1}{q_e} + k_2 t \quad (5)$$

The following equation can be obtained on rearranging the Eq. (5) into a linear form

$$\frac{t}{q_t} = \frac{1}{k_2 q_e^2} + \frac{1}{q_e} t \quad (6)$$

The pseudo-second-order rate constant, k_2 and q_e were calculated from the slope and intercept of the plots t/q_t versus t.

Intraparticle diffusion equation is

$$q_t = k_{id} t^{0.5} \quad (7)$$

A straight line of q_t versus $t^{0.5}$ suggests the applicability of intraparticle diffusion controlling the kinetics of the adsorption and the slope gives the rate constant, k_{if}.

Liquid film diffusion equation is shown as

$$\ln(1 - F) = -k_{fd} t \quad (8)$$

where F is the fractional attainment of equilibrium $F = (q_t/q_e)$, k_{fd} is the rate constant. A linear plot of $-\ln(1 - F)$ versus t with zero intercept would suggest that the adsorption process was controlled by liquid film diffusion.

2.7. Desorption of precious metal ions

Batch desorption experiments were carried out using various concentrations of HCl, NaOH, thiourea–HCl and KCN–NaOH solutions. The adsorbed precious metal ions (100 mg/l) onto LMCCR were washed with EP water several times and transferred into stoppered reagent bottles. To this 30 ml of the desorption agent was added, and then the bottles were shaken at room temperature (30 ± 1 °C) using mechanical shaker for 4 h. The concentration of precious metal ion released from the LMCCR into aqueous phase was analyzed by ICP-AES.

3. Results and discussion

3.1. Characteristics of the adsorbent

The FT-IR spectra of CCR, LMCCR and Pt(IV), Pd(II), Au(III) adsorbed onto LMCCR are shown in Fig. 2. As seen from Fig. 2, in all spectrums the adsorption band around 3420 cm^{-1}, revealing the stretching vibration of N–H group bonded with O–H group in chitosan, and at 1661 cm^{-1} confirms the N–H scissoring from the primary amine, due to the free amino groups in the crosslinked chitosan [28,19]. In Fig. 2e, it was observed that the increasing intensity at 1661 cm^{-1}. Also, the new peak appeared at 1601 cm^{-1}, corresponding to the characteristic

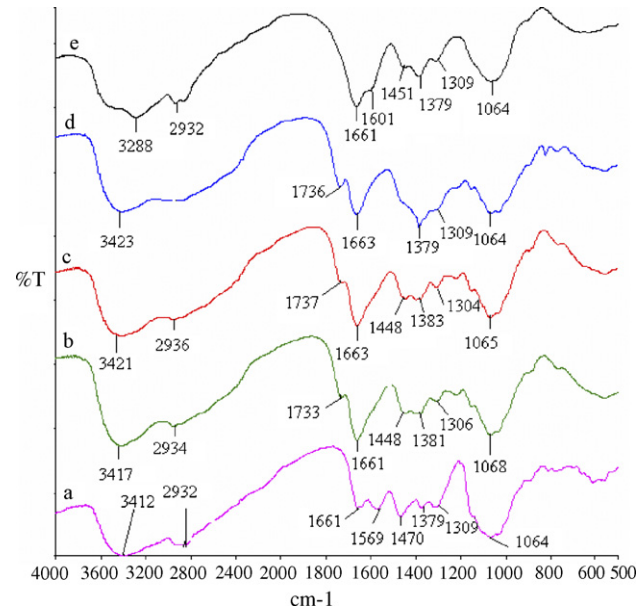

Fig. 2. FT-IR spectra: CCR (a); Pt (b), Au (c), Pd (d) and LMCCR (e) adsorbed onto LMCCR, respectively.

absorption of C=O group in L-lysine. These findings were confirmed that L-lysine was successfully attached to CCR. The band around 1065 cm^{-1} is attributed to the combined effects of C–N stretching vibration of primary amines and the C–O stretching vibration from the primary alcohol in chitosan. The decreasing intensity around 1065 cm^{-1} in Fig. 2b–d was observed for C–N stretching vibration in primary amines and C–O stretching vibration in primary alcohol, indicating that the chemical interaction of Pt(IV), Pd(II) and Au(III) with amino groups in LMCCR [9]. It is predicted that nitrogen atoms are the main adsorption cites for Pt(IV), Pd(II) and Au(III) and also the possibility that the oxygen atoms in the C–O groups in chitosan are involved in precious metal adsorption as well. The disappearance of peak at 1601 cm^{-1}, and new peak appeared around 1737 cm^{-1} in Fig. 2b–d also supports the chemical interactions of Pt(IV), Pd(II) and Au(III) with LMCCR. SEM micrographs of CCR and LMCCR are shown in Fig. 3. As seen from Fig. 3, the morphologies of both resins are different. Also, the modification with L-lysine (Fig. 3b) made the surface is more visible porous than that of CCR.

The ion exchange capacity [29] and BET surface area values for LMCCR were found to be 4.58 meq/g and 82.4 m^2/g, respectively. The obtained ion exchange capacity and surface area values were higher than that of CCR. The substitution of L-lysine on CCR was found to be 4.76 mmol/g.

3.2. Effect of pH

The effect of pH on the adsorption of Pt(IV), Pd(II) and Au(III) was studied individually by varying the pH of 20 mg/l initial metal concentration for a fixed adsorbent dosage of 3.33 g/l at 30 °C and the results are presented in Fig. 4. The results demonstrated that the maximum adsorption capacity was occurred at pH 1.0 for Pt(IV), at pH 2.0 for Au(III) and Pd(II).

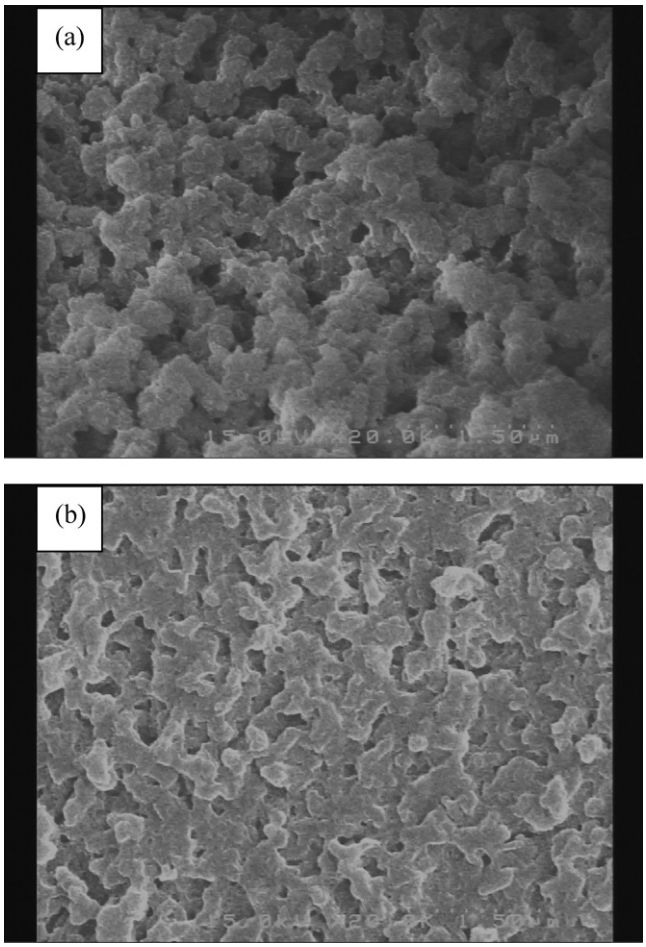

Fig. 3. SEM images of CCR (a) 15 kV × 20,000 and LMCCR (b) 15 kV × 20,000.

The data indicated that the adsorption percentage was slightly changed between pH 1.0–4.0, later it was declined drastically for tested precious metal ions. At low pH, when the solution pH was controlled by HCl, the amount of chloride in the solution is high enough to favor the formation of chloro-anioinc spices that will be adsorbed on protanated amine groups of LMCCR [4]. Moreover, the protanation of amine groups on the LMCCR induced an electrostatic attraction of anionic metal complexes and increased the number of available binding sites for precious metal ions uptake. At acidic solutions the adsorption mechanism of Pt(IV), Pd(II) and Au(III) on LMCCR is assumed to be electrostatic attraction and ion exchange. In the presence of chloride ions the interaction between metal anions and active cites of the LMCCR are shown bellow.

$$\text{R-NH}_2 + \text{H}^+\text{Cl}^- \rightarrow \text{RNH}_3{}^+\text{Cl}^-$$

$$2\text{RNH}_3{}^+\text{Cl}^- + \text{PtCl}_6{}^{2-} \rightleftharpoons (\text{RNH}_3{}^+)_2\text{PtCl}_6{}^{2-} + 2\text{Cl}^-$$

$$2\text{RNH}_3{}^+\text{Cl}^- + \text{PdCl}_4{}^{2-} \rightleftharpoons (\text{RNH}_3{}^+)_2\text{PdCl}_4{}^{2-} + 2\text{Cl}^-$$

$$2\text{RNH}_3 + \text{Cl}^- + \text{AuCl}_4{}^- \rightleftharpoons (\text{RNH}_3{}^+)_2\text{AuCl}_4{}^- + 2\text{Cl}^-$$

At higher pH values decrease the sorption capacity may be explained by the presence of less-adsorbable Pt(IV), Pd(II) and Au(III) species because of the lower availability of chloride anions. Previous results also indicated that higher adsorption capacity for precious metal ions was obtained at pH 1.0–4.0 [16,30–32]. Doker et al. [30] suggested that lower pH values are really important for the precious metal ion recovery in order to eliminate the adsorption of other metal ions.

3.3. Effect of agitation time and initial concentration

Fig. 5 shows the effect of agitation period on the adsorption of Pt(IV), Pd(II) and Au(III) by LMCCR. The results demonstrated that the adsorption increases with increase in agitation time and attained the equilibrium at around 120 min for Pt(IV), Pd(II) and Au(III). An adsorbent with faster uptake is better for the removal of heavy metals. The figure reveals that over 75% adsorption was occurred within 30 min and the equilibrium was attained within 120 min. Experimental studies were carried out with varying initial metal ion concentrations of Pt(IV), Pd(II) and Au(III), ranging from 20 to 200 mg/l using 3.33 g/l

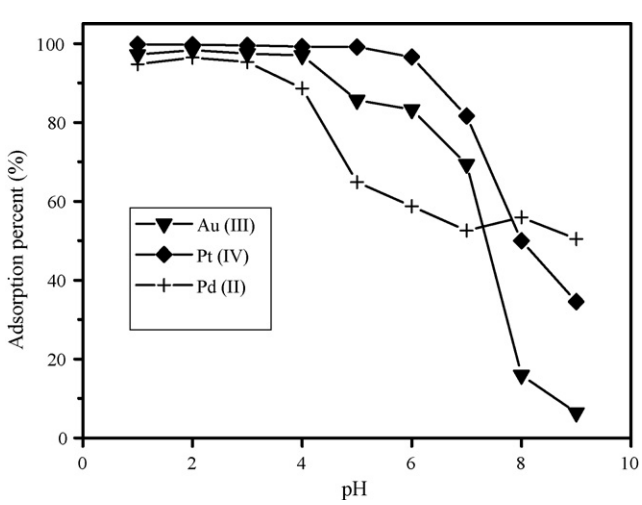

Fig. 4. Effect of pH on adsorption of Pt(IV), Pd(II) and Au(III). Conditions: initial metal ion concentration 20 mg/l, contact time 4 h, adsorbent dose 0.1 g.

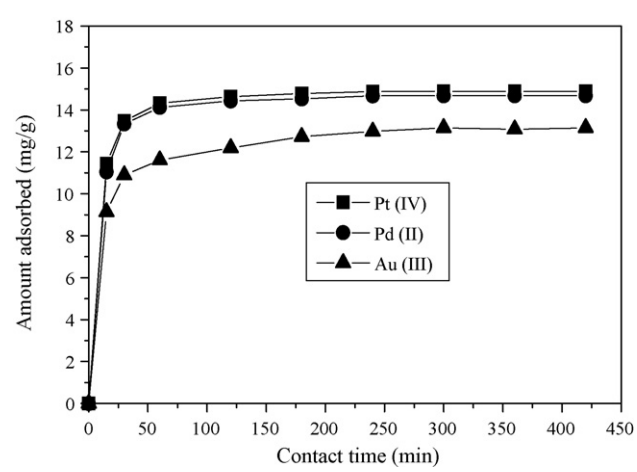

Fig. 5. Effect of contact time on the adsorption of Pt(IV), Pd(II) and Au(III) onto LMCCR. Conditions: initial metal ion concentration 50 mg/l, solution pH 1.0 for Pt(IV) and pH 2.0 for Au(III) and Pd(II), adsorbent dose 0.1 g.

Table 1
Freundlich and Langmuir isotherm constants

	Pt(IV)		Pd(II)		Au(III)	
	LMCCR	CCR	LMCCR	CCR	LMCCR	CCR
Langmuir						
Q_m (mg/g)	129.255	81.942	109.467	101.082	70.341	47.304
b (l/mg)	0.303	1.322	1.579	1.453	0.017	1.081
R^2	0.9983	0.9703	0.9216	0.9029	0.9947	0.9727
Freundlich						
k_F (mg/g)	35.271	30.342	47.471	50.562	3.155	3.032
n	2.572	2.862	3.849	2.741	1.756	4.322
R^2	0.9416	0.9345	0.7948	0.8259	0.9715	0.8164

of adsorbent dose at pH 1.0 for Pt(IV), at pH 2.0 for Au(III) and Pd(II) (the results are not shown in Fig. 5). The results demonstrated that the amount of Pt(IV), Pd(II) and Au(III) adsorbed increases with increasing metal ion initial concentration and also the adsorption percentage decreases with increasing initial metal ion concentration. This is due to the total available sites are limited at fixed adsorbent dose, thereby adsorbing almost the same amount of solute, resulting in a decreasing of percentage adsorption corresponding to an increase in initial metal ion concentration. It is very clear from these results that the agitation time is required for maximum uptake of metal ions by LMCCR was dependent on the initial metal ion concentration. Based on these results, the agitation time was fixed about 4 h for rest of the batch experiments.

3.4. Adsorption isotherms

The experimental adsorption data was compared with Freundlich and Langmuir isotherm models. The Langmuir isotherm is based on the monolayer adsorption on the active sites of the adsorbent. On the other hand, the Freundlich isotherm explains the adsorption on a heterogeneous (multiple layer) surface with uniform energy. The experimental adsorption capacity and the adsorption capacity predicted by the both Langmuir and Freundlich models are shown in Fig. 6, the corresponding Langmuir and Freundlich parameters along with regression coefficients are listed in Table 1. The experimental data obtained for the adsorption of Pt(IV), Pd(II) and Au(III) on CCR plotted with Langmuir and Freundlich isotherm models are not shown graphically, but the isotherm constants are presented in Table 1. The results presented in Table 1 suggest that the maximum adsorption capacity obtained for Pt(IV), Pd(II) and Au(III) on LMCCR is higher than that of CCR. This is because of the incorporation of L-lysine in CCR is assumed to produce more amine groups to interact with Pt(IV), Pd(II) and Au(III) ions, which enhances the adsorption capacity. The grafting of N-groups increases the number of sorption sites in LMCCR. Also, the higher surface area and ion exchange capacity of LMCCR when compared to that of CCR may enhance the sorption capacity. Other reasons may be (a) to increase the density of sorption sites and (b) to change the sorption sites in order to increase sorption capacity of LMCCR. As can be seen from Fig. 6, the fit is better with Langmuir model than with Freundlich model. Based on the highest regression coefficient value of Langmuir isotherm was suggesting that the present adsorption process probably dominated by a monolayer adsorption process rather than a multiple adsorption one. The adsorption capacity obtained for Pt(IV) is higher

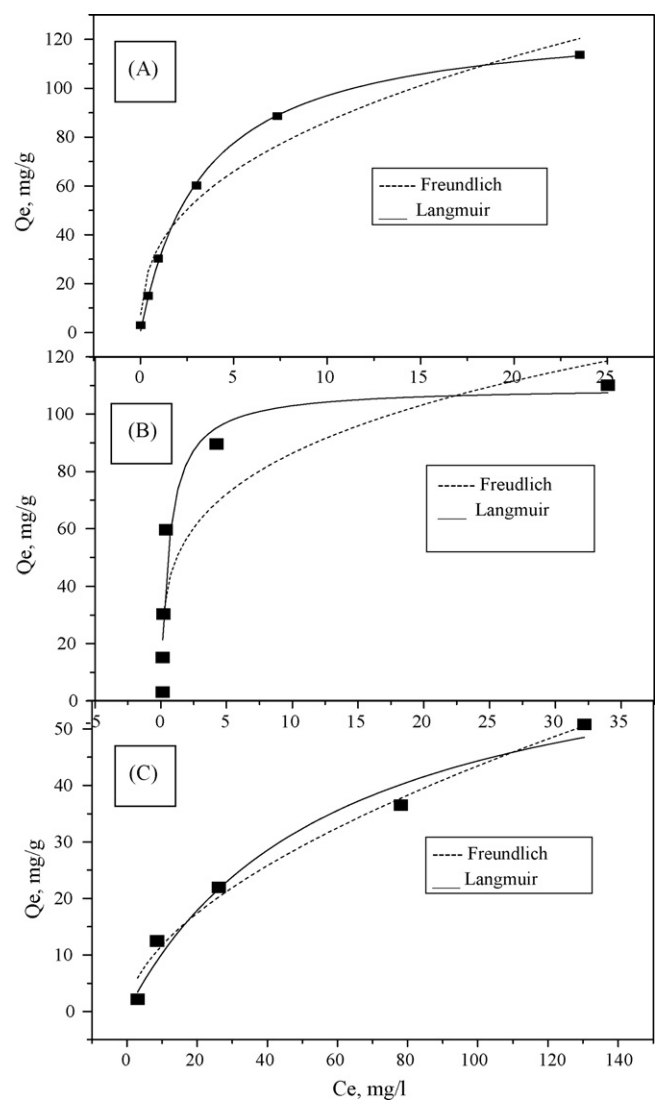

Fig. 6. Adsorption isotherms of platinum (A), palladium (B) and gold (C) at 30 °C. Conditions—initial metal ion concentration: 10–400 mg/l; solution pH 1.0 for Pt(IV) and pH 2.0 for Au(III) and Pd(II); adsorbent dose: 0.1 g; contact time: 4 h.

Table 2
Maximum adsorption capacities for the adsorption of Pt(IV), Pd(II) and Au(III) onto various adsorbents

Adsorbent	Adsorption capacity (mg/g)			Reference
	Pt(IV)	Pd(II)	Au(III)	
N-carboxymethyl chitosan			33.90	[36]
Bayberry tannin immobilized collagen fiber membrane	45.8	33.4		[29]
Thiol cotton fiber		32–42[a]	64–68[a]	[37]
Fe_3O_4 nano-particles	13.266	10.959		[38]
Alfalfa biomass			35.972	[39]
EN-Lignin	104.57	22.66	606.76	[40]
PA-Lignin	42.93	40.43	384	[40]
Amberlite IRC 718	66.334	58.52	135.93	[41]
Amberlite XAD-16		33.56		[42]
Poly(vinylbenzylchloride–acrylonitryle–divinylbenzene) modified with tris(2-aminoethyl)amine	245	280	190	[43]
Lysine modified crosslinked chitosan resin	129.26	109.47	70.34	This work

[a] Ten batches adsorption capacities range.

when compared to Pd(II) and Au(III), showing the following order: Pt(IV) > Pd(II) > Au(III). The higher adsorption capacity of Pt(IV) should be due to the higher interaction activity with LMCCR at acidic pH condition.

Table 2 compares the adsorption capacity of different types of adsorbents [36–43] using for Pt(IV), Pd(II) and Au(III) adsorption. The adsorption capacity of LMCCR was relatively high when compared to several other adsorbents. The differences of precious metal ion uptake on various adsorbents are due to the properties (function groups, surface area, particle size, etc.) of the adsorbents.

The essential features of the Langmuir isotherm can be expressed in terms of the dimensionless equilibrium parameter R_L, which is defined as $R_L = 1/(1 + bC_0)$, where b is the Langmuir constant and C_0 is the initial concentration of Pt(IV), Pd(II) and Au(III). According to Hall et al. [33], R_L values within the range $0 < R_L < 1$, indicate favorable adsorption. The present adsorption system R_L values between the 0 and 1, the values are presented in Table 3. This means that the adsorption of Pt(IV), Pd(II) and Au(III) on LMCCR is favorable and useful for the removal of precious metal ions.

3.5. Adsorption kinetics

In order to evaluate the kinetic mechanism that controls the adsorption process, the pseudo-first-order, pseudo-second-order, intraparticle diffusion and liquid film diffusion models were tested to interpret the experimental data. The kinetic models for Pt(IV), Pd(II) and Au(III) are presented in Figs. 7–10 and the results of kinetic parameters are shown in Table 4 and Table 5.

Table 3
R_L values based on the Langmuir equation

C_0 (mg/l)	Pt ($\times 10^{-2}$)	Pd ($\times 10^{-2}$)	Au ($\times 10^{-2}$)
10	0.1431	0.0594	2.8011
50	0.0286	0.0119	0.5731
100	0.0143	0.0059	0.2874
200	0.0072	0.0030	0.1439
300	0.0048	0.0020	0.0960
400	0.0036	0.0015	0.0720

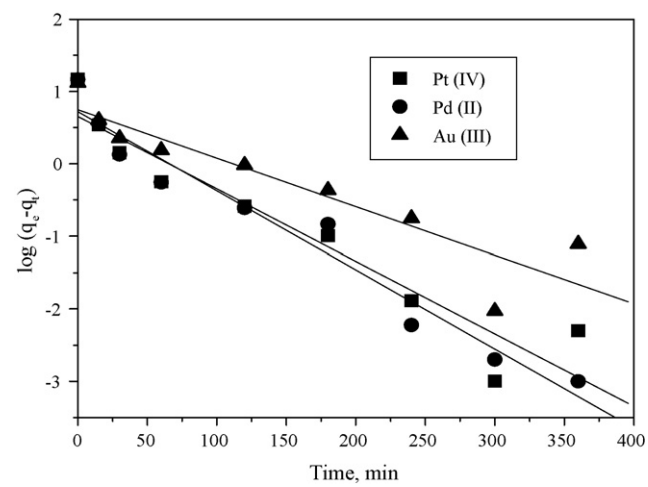

Fig. 7. Lagergren plots for the adsorption of Pt(IV), Pd(II) and Au(III) onto LMCCR.

As shown in Table 4, the correlation coefficient values of pseudo-second-order model were higher than that of pseudo-first-order model. Also, the calculated q_e values from pseudo-second-order model were very close to experimental q_e values. In the case

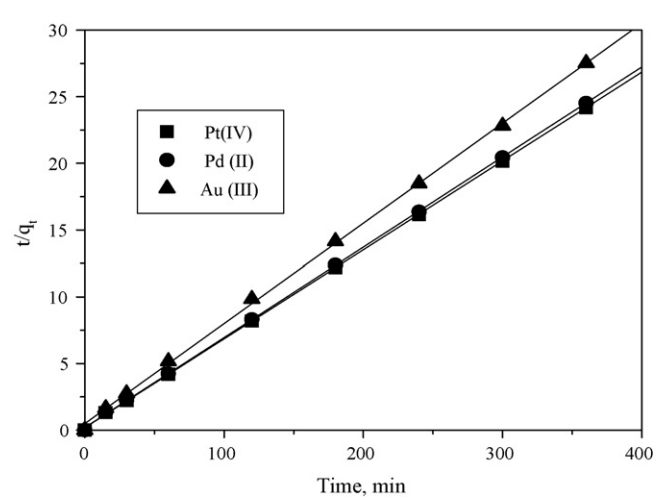

Fig. 8. Pseudo-second-order kinetic model for the adsorption of Pt(IV), Pd(II) and Au(III) onto LMCCR.

Table 4
Comparison of pseudo-first-order and pseudo-second-order rate constants and calculated and experimental q_e values

Metal	q_e (exp) (mg/g)	Pseudo-first-order kinetics			Pseudo-second-order kinetics			
		k_1 (min^{-1})	q_e (cal) (mg/g)	R^2	k_2 (g/mg min)	h (mg/g min)	q_e (cal) (mg/g)	R^2
Pt(IV)	14.886	0.01	4.525	0.9154	0.0624	5.678	14.992	0.9999
Pd(II)	14.721	0.0109	5.261	0.9591	0.0185	5.399	14.793	0.9999
Au(III)	13.152	0.0067	5.601	0.8477	0.0059	2.069	13.315	0.9996

Table 5
Intraparticle diffusion rate constant and liquid film diffusion rate constant for the adsorption of Pt(IV), Pd(II) and Au(III) onto LMCCR

Metal	Intraparticle diffusion			Liquid film diffusion		
	k_{id} (mg/g min$^{0.5}$)	Intercepts	R^2	k_{fd} (min^{-1})	Intercepts	R^2
Pt(IV)	1.51×10^{-1}	12.32	0.7882	2.14×10^{-2}	1.61	0.9564
Pd(II)	1.54×10^{-1}	12.06	0.7746	2.40×10^{-2}	1.40	0.9779
Au(III)	2.04×10^{-1}	9.50	0.9069	1.23×10^{-2}	1.27	0.9851

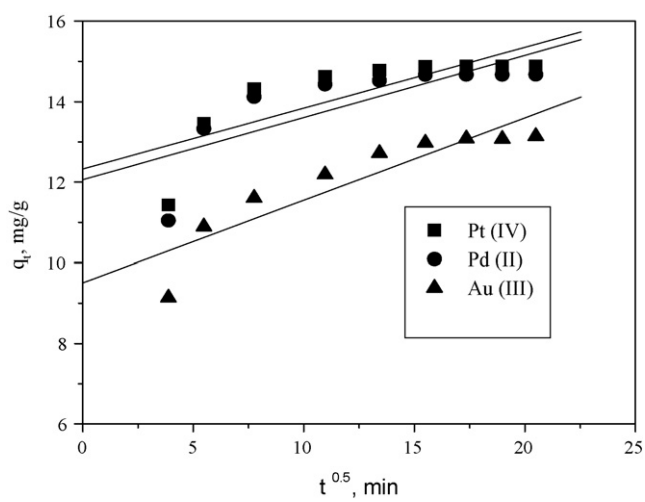

Fig. 9. Intrapraticle diffusion model for the adsorption of Pt(IV), Pd(II) and Au(III) onto LMCCR.

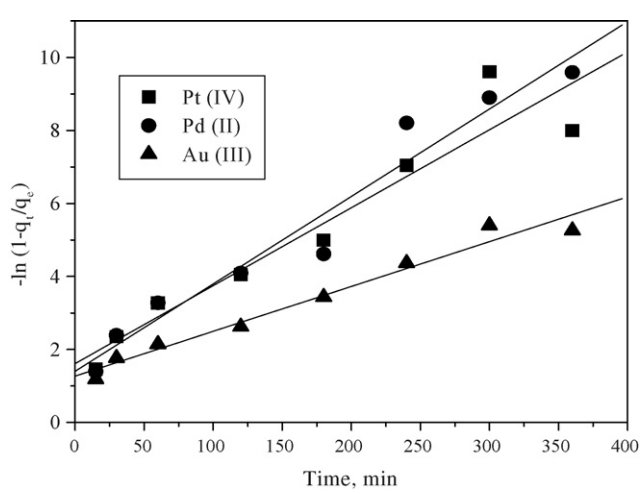

Fig. 10. Liquid film diffusion model for the adsorption of Pt(IV), Pd(II) and Au(III) onto LMCCR.

of pseudo-first-order model the calculated q_e values differed severely from the experimental q_e values. The adsorption data was processed to determine weather intraparticle diffusion is the rate-limiting step. The plots obtained in Fig. 9 showed that multi linearity with different stages of adsorption. As seen from Fig. 9, the straight line did not pass through the origin and this further indicated that the intraparticle diffusion may not the rate-controlling step. Weather the process of adsorption is controlled by liquid film diffusion, the adsorption data was tested by plotting the $-\ln(1-F)$ versus t. Although the plots were linear they do not pass through the origin and the intercepts varies from 1.27 to 1.61 (Fig. 10). Therefore, the liquid film diffusion model may not be the controlling factor in determining the kinetics of the process. Based on the higher correlation coefficients and the agreement of calculated q_e values with experimental values the adsorption of Pt(IV), Pd(II) and Au(III) onto LMCCR was best described by pseudo-second-order equation. This suggests that the second order kinetic model based on the assumption that the rate limiting step may be chemical sorption and not involving mass transfer in solution. It is more likely to predict that the adsorption behavior may involve valency forces through sharing of electrons between precious metal cations and adsorbent. The pseudo-second-order rate constant (k_2) and initial sorption rate (h) for Pt(IV) were higher when compared to Pd(II) and Au(III). In many cases, the pseudo-second-order kinetic model provided better results on the adsorption of Fe on chitosan and crosslinked chitosan beads [1], Cu, Cd and Ni on chemically modified chitosan [20], Cr and Cu ions on chitosan [34].

The magnitude of activation energy (E_a) can give an idea about weather the adsorption process is physical or chemical. The activation energy of the adsorption process was calculated by Arrhenius equation.

$$k = A \exp\left(\frac{-E_a}{RT}\right)$$

where k is the pseudo-second-order rate constant of sorption (g/mg min), A the Arrhenius constant which is a temperature independent factor (g/mg min), E is the activation energy of

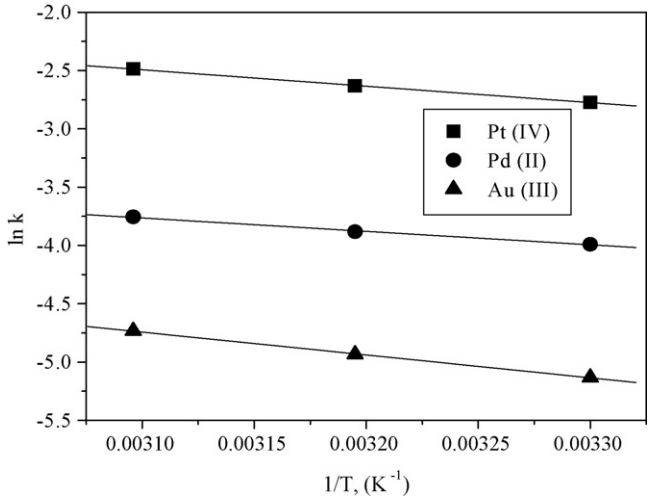

Fig. 11. Relationship between ln k and $1/T$ for LMCCR.

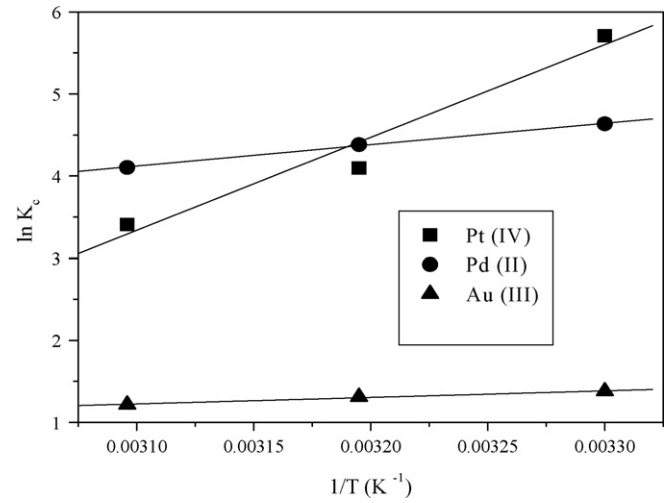

Fig. 12. Van't Hoff plots for the adsorption of Pt(IV), Pd(II) and Au(III) onto LMCCR. Conditions: initial metal ion concentration: 100 mg/l; solution pH 1.0 for Pt(IV) and pH 2.0 for Au(III) and Pd(II); adsorbent dose: 0.1 g; contact time: 4 h; temperature: 30–50 °C.

sorption (kJ/mol), R is the gas constant (8.314 J/mol K) and T is the absolute temperature (K). A straight line with slope $-E_a/R$ of ln k versus $1/T$ is obtained.

In physical adsorption the energy requirements are small and the activation energy usually not more than 4.2 kJ/mol, because the forces involved in physical adsorption are usually weak [35]. However, chemical adsorption is specific and involves forces much stronger than in physical adsorption. Fig. 11 shows the values of ln k versus T were plotted for the adsorption of 50 mg/l Pt(IV), Pd(II) and Au(III) onto LMCCR. The obtained E_a values for LMCCR are 11.71, 9.56 and 16.29 kJ/mol for Pt(IV), Pd(II) and Au(III), respectively. This suggests that the adsorption of Pt(IV), Pd(II) and Au(III) on LMCCR is chemical adsorption.

3.6. Effect of temperature

The effect of temperature on adsorption of Pt(IV), Pd(II) and Au(III) ions by LMCCR was studied using 100 mg/l initial metal concentration at 30, 40 and 50 °C. The results found that the adsorption capacity decreased with increasing temperature. This indicates that the adsorption process is exothermic in nature. The thermodynamic parameters such as change in free energy (ΔG°), enthalpy (ΔH°) and entropy (ΔS°) were calculated from the following equations:

$$\Delta G^\circ = -RT \ln K_c$$

$$K_C = \frac{C_{Ae}}{C_e}$$

$$\log K_c = \frac{\Delta S^\circ}{2.30R} - \frac{\Delta H^\circ}{2.303RT}$$

where R is the gas constant, K_c is the equilibrium constant, T is the temperature (in K), C_{Ae} is the equilibrium concentration of Pt(IV), Pd(II) and Au(III) on adsorbent (mg/l), and C_e is the equilibrium concentration of Pt(IV), Pd(II) and Au(III) in the solution (mg/l). The values of ΔH° and ΔS° were calculated from the slope and intercept of the Van't Hoff linear plots (Fig. 12) of $\log K_c$ versus $1/T$. The results are presented in Table 6. The negative values of ΔG° indicates that the spontaneous nature of adsorption. As the temperature increases, the ΔG° values decrease, indicating less driving force and hence

Table 6
Thermodynamic parameters for the adsorption of Pt(IV), Pd(II) and Au(III) onto LMCCR

Metal	Temperature (°C)	Thermodynamics			
		ΔG (kJ/mol)	ΔH (kJ/mol)	ΔS (J/mol K)	R^2
Pt(IV)	30	−14.385	−94.181	−264.202	0.973
	40	−10.906			
	50	−9.147			
Pd(II)	30	−11.679	−21.683	−32.946	0.9981
	40	−11.404			
	50	−11.020			
Au(III)	30	−3.473	−6.617	−10.331	0.9877
	40	−3.41			
	50	−3.265			

Table 7
Desorption data of Pt(IV), Pd(II) and Au(III)

Desorption agent	Desorption efficiency (%)		
	Pt(IV)	Pd(II)	Au(III)
HCl			
0.5 M HCl	19.64	3.18	32.13
1 M HCl	28.12	4.45	53.72
2 M HCl	39.32	6.42	62.21
5 M HCl	38.22	6.74	65.87
Thiourea–HCl			
0.1 M Thiourea–2 M HCl	47.38	51.25	50.36
0.3 M Thiourea–2 M HCl	70.28	68.26	73.41
0.5 M Thiourea–2 M HCl	92.16	94. 12	95.16
0.7 M Thiourea–2 M HCl	97.21	99.98	99.82
1 M Thiourea–2 M HCl	98.62	99.28	99. 86
NaOH			
0.1 M NaOH	26.32	8.64	2.07
0.3 M NaOH	44.37	9.73	2.62
0.5 M NaOH	62.18	10.78	2.92
1 M NaOH	63.34	10.83	3.06
KCN–NaOH			
0.1 M KCN–0.5 M NaOH	49.63	46.28	38.24
0.5 M KCN–0.5 M NaOH	90.26	92.18	75.26
1 M KCN–0.5 M NaOH	98.22	99.44	88.93
1.5 M KCN–0.5 M NaOH	98.66	99.24	90.12

resulting lesser adsorption capacity at higher temperatures. The negative values of ΔH° and ΔS° confirms the exothermic nature and the decreased randomness at the solid/solute interface during the adsorption of Pt(IV), Pd(II) and Au(III), respectively.

3.7. Desorption studies and reuse

To achieve the practical adsorption, the adsorbate has to be desorbed and spend adsorbent reused. In the present study the desorption efficiency of adsorbed precious metals (100 mg/l) onto LMCCR was studied by various concentrations of 30 ml HCl, NaOH, thiourea–HCl and KCN–NaOH solutions. The systematic influences of these desorbing solutions on adsorbed precious metals onto LMCCR are shown in Table 7. The results show that 0.7 M thiourea–2 M HCl solution can effectively desorbed the Pt(IV), Pd(II) and Au(III) (nearly 100%) metal ions from adsorbent material. The high percentage of desorption obtained when 0.7 M thiourea–2 M HCl solution was used may be explained by both stable complexes and the electrostatic interactions between the Pt(IV), Pd(II) and Au(III) species and charged species from elution, through the comparison of the electric double layer, which would weaken the interaction between the adsorbent and precious metal ions, promoting desorption. As seen from Table 7, KCN–NaOH reagent solution also provided better results for the desorption of tested precious metal ions. But it is not advisable to use KCN reagent for the desorption studies, due to its acute toxicity. The low recoveries caused by HCl and NaOH, due to the chelating mechanism involved in the metal adsorption process.

The stability and the potential regeneration of the adsorbent were investigated. The adsorbent can be reused after desorption with 0.7 M thiourea–2 M HCl solution. The results provided that the adsorbent was stable without loss of the adsorption capacity up to at least 5 cycles (data not shown). Because of the EDGE crosslinker in the resin, it enhances the stability against acidic or alkaline solutions. Previous studies also reported that the crosslinking step enhanced the stability of chitosan against acid, alkali and chemicals [1,5].

3.8. Preconcentration and recovery

The sample solution containing the Pt(IV), Pd(II) and Au(III) in the concentration (0.05–10 μg/l), and the pH was adjusted to desired value with HCl or ammonia solution. The solution was passed through the micro-column (20 mm × 3.0 mm i.d.) containing 0.1 g of LMCCR, at a flow rate of 1.0 ml/min. Then the column was rinsed with 5 ml of EP water. Afterwards, the retained metal ions were eluted with 5 ml of 0.7 M thiourea–2.0 M HCl solution at a flow rate of 1.0 ml/min. The concentrations of the analytes were determined by ICP-AES. From the measured results, recovery was found to be more than 98% for all tested precious metal ions. The preconcentration factor for the metal ions with LMCCR was also studied. The results show that the preconcentration factor for Pt(IV), Pd(II) and Au(III) were 200, 190 and 170, respectively.

3.9. Effect of coexisting ions

The effects of common coexisting ions on the adsorption of Pt(IV), Pd(II) and Au(III) (30 ml, 1.0 μg/ml) on LMCCR were studied. The results indicate that the maximum tolerance limits are 20,000 μg/ml for Cl^-, NO_3^-, SO_4^{2-}; 10,000 μg/ml for CH_3COO^-; 30,000 μg/ml for Ca^{2+}, Mg^{2+}; 40,000 and 50,000 μg/ml for K^+, Na^+ ions. The results indicates that various cations and anions present in water samples has no obvious influence on the determination of tested precious metal ions under the reported conditions and the LMCCR has a good selectivity for the adsorption of Pt(IV), Pd(II) and Au(III) ions.

4. Conclusions

The study indicated that L-lysine modified crosslinked chitosan as an effective adsorbent for the adsorption of Pt(IV), Pd(II) and Au(III) from aqueous solutions. The results demonstrated that the adsorption process is dependent on contact time, initial metal ion concentration, solution pH and temperature. The adsorption capacity of LMCCR is higher than that of CCR. The maximum adsorption capacity was obtained at pH 1.0 for Pt(IV), at pH 2.0 for Au(III) and Pd(II). By working at low pH values, unwanted matrix effects were eliminated without adding any matrix. For all studied systems of kinetics, the pseudo-second-order model provides better correlation of the adsorption data than the pseudo-first-order model; this suggests that the rate-limiting step may be chemical sorption. The adsorption isotherms could be well fitted by the Langmuir isotherm equation. The negative values of enthalpy confirm the exothermic

nature of adsorption. The results showed that the adsorption behavior of precious metal ions on LMCCR was not affected by the physical adsorption, but was mainly dependent on the chemical interaction.

Acknowledgments

One of the authors Dr. A. Ramesh, expressed his sincere thanks to Japan Society for the Promotion of Science (JSPS), Japan for providing the financial assistance in the form a fellowship. This research was partly supported by a Grant-in-Aid (No. 18550138) from the JSPS.

References

[1] W.S.W. Nagh, S.A. Ghani, A. Kamari, Adsorption behavior of Fe (II) and Fe (III) ions in aqueous solution on chitosan and crosslinked chitosan beads, Bioresour. Technol. 96 (2005) 443–450.

[2] R.A.A. Muzzarelli, R. Rocchetti, Enhanced capacity of chitosan for transition-metal ions in sulphate-sulphuric acid solutions, Talanta 21 (1974) 1137–1143.

[3] J.R. Evans, W.G. Davids, J.D. MacRae, A. Amirbahman, Kinetics of cadmium uptake by chitosan-based crab shells, Water Res. 36 (2002) 3219–3226.

[4] P. Ghassary, T. Vincent, J.S. Marcano, L.E. Macaskie, E. Guibal, Palladium and platinum recovery from bicomponent mixtures using chitosan derivatives, Hydrometallurgy 76 (2005) 131–147.

[5] E. Guibal, Interactions of metal ions with chitosan-based sorbents: a review, Sep. Purif. Technol. 38 (2004) 43–74.

[6] T.Y. Hsein, G.L. Rorer, Heterogeneous crosslinking of chitosan gel beads: kinetics, modeling, and influence on cadmium ion adsorption capacity, Ind. Eng. Chem. Res. 36 (1997) 3631–3638.

[7] O.A.C.J. Monteiro, C. Airoldi, Some studies of crosslinking chitosan–glutaraldehyde interaction in a homogeneous system, Int. J. Biol. Macromol. 26 (1999) 119–128.

[8] G. Rojas, J. Silva, J.A. Flores, A. Rodriguez, M. Ly, H. Maldonodo, Adsorption of chromium onto crosslinked chitosan, Sep. Purif. Technol. 44 (2005) 31–36.

[9] R.S. Vieira, M.M. Beppu, Interaction of natural and crosslinked chitosan membranes with Hg(II) ions, Colloids Surf. A 279 (2006) 196–207.

[10] R.S. Juang, C.Y. Ju, Kinetics of sorption of Cu (II)-ethylenediaminetetraacetic acid chelated anions on crosslinked, polyaminated chitosan beads, Ind. Eng. Chem. Res. 37 (1998) 3463–3469.

[11] Y.H. Gao, K. Oshita, K.H. Lee, S. Motomizu, Development of column-pretreatment chelating resins for matrix elimination/multi-element determination by inductively coupled plasma-mass spectrometry, Analyst 127 (2002) 1713–1719.

[12] G. Paradossi, F. Cavalieri, V. Crescenzi, ^{1}H NMR relaxation study of a chitosan-cyclodextrin network, Carbohydr. Res. 300 (1997) 77–84.

[13] M. Ruiz, A.M. Sastre, E. Guibal, Pd and Pt recovery using chitosan gel beads. II. Influence of chemical modifications on sorption properties, Sep. Sci. Technol. 37 (2002) 2385–2403.

[14] Y. Kuvamura, H. Yosidha, S. Asai, H. Tanibe, Breakthrough curve for adsorption of mercury (II) on polyaminated highly porous chitosan beads, Water Sci. Technol. 35 (1997) 97–105.

[15] M. Ruiz, A.M. Sastre, E. Guibal, Osmium and iridium sorption on chitosan derivatives, Solv. Extr. Ion Exch. 21 (2003) 307–329.

[16] E. Guibal, N. Van Offenberg Sweeney, T. Vincent, J.M. Tobin, Sulfur derivatives of chitosan for palladium sorption, React. Funct. Polym. 50 (2002) 149–163.

[17] A. Sabaruddin, K. Oshita, M. Oshima, S. Motomizu, Synthesis of chitosan resin possessing 3,4-diamino benzoic acid moiety for the collection/concentration of arsenic and selenium in water samples and their measurement by inductively coupled plasma-mass spectrometry, Anal. Chim. Acta 542 (2005) 207–215.

[18] A. Sabaruddin, K. Oshita, M. Oshima, S. Motomizu, Synthesis of crosslinked chitosan possessing *N*-methyl-D-glucamine moiety (CCTS-NMDG) for adsorption/concentration of boron in water samples and its accurate measurement by ICP-MS and ICP-AES, Talanta 66 (2005) 136–144.

[19] R.K. Katarina, T. Takayanagi, M. Oshima, S. Motomizu, Synthesis of a chitosan-based chelating resin and its application to the selective concentration and ultratrace determination of silver in environmental water samples, Anal. Chim. Acta 558 (2006) 246.

[20] K.C. Justi, V.T. Favere, M.C.M. Laranjeria, A. Neves, R.A. Peratla, Kinetics and equilibrium adsorption of Cu (II), Cd (II), and Ni (II) ions by chitosan functionalized with 2[-bis-(pyridylmethyl)aminomethyl]-4-methyl-6-formylphenol, J. Colloid Interf. Sci. 291 (2005) 369–374.

[21] H. Freundlich, Uber die adsorption in losungen, Z. Phys. Chem. 57 (1906) 387–470.

[22] I. Langmuir, The adsorption of gases on plane surface of glass, mica and platinum, J. Am. Chem. Soc. 40 (1918) 1361–1368.

[23] S. Lagergren, Zur theorie der sogenannten adsorption geloster stoffe, Kungliga Svenska Vetenskapsakadomiens Handlinger 24 (1898) 1–39.

[24] Y.S. Ho, G. McKay, The sorption of dye from aqueous solution by peat, Chem. Eng. J. 70 (1998) 115–124.

[25] Y.S. Ho, G. McKay, Pseudo-second-order model for sorption processes, Process Biochem. 34 (1999) 451–465.

[26] W.J. Weber, J.C. Morris, Kinetics of adsorption of carbon from solutions, J. Sanit. Eng. Div. Am. Soc. Civ. Eng. 89 (1963) 31–63.

[27] G.E. Boyd, A.W. Adamson, L.S. Myers, The exchange adsorption of ions from aqueous solutions by organic zeolites. 11. Kinetics, J. Am. Chem. Soc. 67 (1949) 2836–2848.

[28] R. Tang, Y. Du, L. Fan, Dialdehyde starch-crosslinked chitosan films and their antimicrobial effects, J. Polym. Sci. B 41 (2003) 993–997.

[29] K. Takeda, F. Kawakami, M. Sasaki, Ion-exchange equilibrium behavior of complex ions in Fe^{3+}-Cl^- and $UO_2{}^2$–Cl^- systems, Nihonkagakukaishi 2 (1984) 1138–1145.

[30] S. Doker, S. Malcı, M. Dogan, B. Salih, New poly(*N*-(hydroxymethyl) methacrylamide-1-allyl-2-thiourea) hydrogels prepared by radiation-induced polymerization: selective adsorption, recovery and pre-concentration of Pt (II) and Pd (II), Anal. Chim. Acta 553 (2005) 73–82.

[31] H.W. Ma, X.P. Liao, X. Liu, B. Shi, Recovery of platinum(IV) and palladium(II) by bayberry tannin immobilized collagen fiber membrane from water solution, J. Membr. Sci. 278 (2006) 373–380.

[32] C. Kavaklı, S. Malcı, S.A. Tuncel, B. Salih, Selective adsorption and recovery of precious metal ions from geological samples by 1,5,9,13-tetrathiacyclohexadecane-3,11-diol anchored poly(*p*-CMS-DVB) microbeads, React. Funct. Polym. 66 (2006) 275–285.

[33] K.R. Hall, L.C. Eagleton, A. Acrivos, T. Vermeulen, Pore and solid diffusion kinetics fixed bed adsorption under constant pattern conditions, Ind. Eng. Chem. Fundam. 5 (1966) 212–223.

[34] Y. Sag, Y. Aktay, Kinetic studies on sorption of Cr(VI) and Cu(II) ions by chitin, chitosan and *Rhizopus arrhizus*, Biochem. Eng. J. 12 (2002) 143–153.

[35] E.I. Unuabonah, K.O. Adebowale, B.I. Olu-Owolabi, Kinetic and thermodynamic studies of the adsorption of lead (II) ions onto phosphate modified kaolinite clay, J. Hazard. Mater. 144 (2007) 386–395.

[36] W.S.W. Ngah, K.H. Liang, Adsorption of gold(III) Ions onto chitosan and *N*-carboxymethyl chitosan: equilibrium studies, Ind. Eng. Chem. Res. 38 (1999) 1411–1414.

[37] M. Yu, D. Sun, W. Tian, G. Wang, W. Shen, N. Xu, Systematic studies on adsorption of trace elements Pt, Pd, Au, Se, Te, As, Hg, Sb on thiol cotton fiber, Anal. Chim. Acta 456 (2002) 147–155.

[38] A. Uheida, M. Iglesias, C. Fontas, M. Hidalgo, V. Salvado, Y. Zhang, M. Muhammed, Sorption of palladium(II), rhodium(III), and platinum(IV) on Fe_3O_4 nanoparticles, J. Colloid Interf. Sci. 301 (2006) 402–408.

[39] G. Gamez, J.L. Gardea-Torresdey, K.J. Tiemann, J. Parsons, K. Dokken, M.J. Yacaman, Recovery of gold(III) from multi-elemental solutions by alfalfa biomass, Adv. Environ. Res. 7 (2003) 563–571.

[40] D. Parajuli, H. Kawakita, K. Inoue, M. Funaoka, Recovery of gold(III), palladium(II), and platinum(IV) by aminated lignin derivatives, Ind. Eng. Chem. Res. 45 (2006) 6405–6412.

[41] C. Park, J.S. Chung, K.W. Cha, Separation and preconcentration method for palladium, platinum and gold from some heavy metals using Amberlite IRC 718 chelating Resin, Bull. Korean Chem. Soc. 21 (2000) 121–124.

[42] A. Tunceli, A.R. Turker, Determination of palladium in alloy by flame atomic absorption spectrometry after preconcentration of its iodide complex on Amberlite XAD-16, Anal. Sci. 16 (2000) 81–85.

[43] D. Jermakowicz-Bartkowiak, B.N. Kolarz, A. Serwin, Sorption of precious metals from acid solutions by functionalised vinylbenzyl chloride–acrylonitryle–divinylbenzene copolymers bearing amino and guanidine ligands, React. Funct. Polym. 65 (2005) 135–142.